Syndiotactic-Specific Radical Polymerization of *N*,*N*-Dimethylacrylamide in the Presence of Tartrates: a Proposed Mechanism for the Polymerization

TOMOHIRO HIRANO, SHUHEI MASUDA, SHOU NASU, KOICHI UTE, TSUNEYUKI SATO

Institute of Technology and Science, Tokushima University, 2-1 Minamijosanjima, Tokushima 770-8506, Japan

Correspondence to : T. Hirano (E-mail: hirano@chem.tokushima-u.ac.jp)

ABSTRACT: Radical polymerization of *N*,*N*-dimethylacrylamide (DMAAm) was investigated in the presence of tartrates, such as diethyl L-tartrate, diisopropyl L-tartrate, and di-*n*-butyl L-tartrate, in toluene at low temperatures. Syndiotactic polymers were obtained in the presence of tartrates, whereas isotactic polymers were obtained in the absence of tartrates. The syndiotactic-specificity increased with increasing amount of tartrates and with decreasing polymerization temperature. NMR analysis suggested that DMAAm and tartrates formed a 1:1 complex through double hydrogen bonding. A mechanism for the syndiotactic-specific radical polymerization of DMAAm is proposed.

Keywords: hydrogen bond; *N*,*N*-dimethylacrylamide; radical polymerization; syndiotactic; stereospecific polymers; tartrates;

INTRODUCTION

Stereospecific radical polymerization is a challenging topic in polymer synthesis and has attracted much attention. In the last decade particularly, stereocontrol of radical polymerization has been reported for a wide range of monomers, including methacrylates,[1-4] vinyl esters,[5] (meth)acrylamides,[6-18] and *N*-vinylamides.[19,20]

We have shown that a hydrogen-bonding interaction is useful for controlling stereospecificity in radical polymerization of vinyl monomers possessing amide moieties. For example, syndiotactic polymers were obtained by radical polymerization of *N*-isopropylacrylamide (NIPAAm) by adding phosphoric acid derivatives such as hexamethylphosphoramide (HMPA),[12] whereas isotactic polymers were obtained with addition of pyridine *N*-oxide (PNO) derivatives such as 3,5-dimethylpyridine *N*-oxide (35DMPNO).[14] NMR analysis revealed that the induced stereospecificity depended on the structure of the hydrogen bond-assisted complexes between NIPAAm and Lewis bases.

In the course of our study, tartrates were found to induce syndiotactic-specificity in the radical polymerization of *N*,*N*-dimethylacrylamide (DMAAm) in toluene at –60°C.[21] The syndiotacticity (r=66%) of the polymer obtained is the highest of radically prepared poly(DMAAm) so far reported, although the syndiotacticity is lower than that of poly(DMAAm) prepared via anionic[22] or

coordination[23] polymerization.

To understand the mechanism of the syndiotactic-specific radical polymerization of DMAAm in the presence of tartrates, in the present study we investigated the radical polymerization of DMAAm in the presence of tartrates in more detail, in addition to the structure of the hydrogen bond-assisted complex.

EXPERIMENTAL

Materials

DMAAm (Tokyo Kasei Kogyo Co.) was fractionally distilled. Toluene was purified by washing with sulfuric acid, water and 5% aqueous NaOH, then fractional distillation. Tri-*n*-butylborane (*n*-Bu_3B) as a THF solution (1.0 M) (Aldrich Chemical Co.), diethyl L-tartrate (L-EtTar), diisopropyl L-tartrate (L-iPrTar), di-*n*-butyl L-tartrate (L-BuTar), diethyl D-tartrate (D-EtTar), and diethyl D-malate (D-EtMal) (Tokyo Kasei Kogyo Co.) were used without further purification. Di-*n*-butyl *meso*-tartrate (*meso*-BuTar) was prepared according to the literature.[24]

Polymerization

A typical polymerization procedure was as follows. DMAAm (0.261 g, 2.64 mmol) was dissolved in toluene to prepare 5 mL of solution (0.528 mol L^{-1}). Four milliliters of the solution was transferred to a glass ampoule and cooled to –60°C. Polymerization was initiated by adding *n*-Bu_3B solution (0.21 mL) to the monomer solution.[25] After 24 h, the reaction was terminated by adding a small amount of a solution of

2,6-di-*t*-butyl-4-methylphenol in THF at –60°C. The polymerization mixture was poured into a large amount of diethyl ether, the precipitated polymer collected by filtration or centrifugation, and dried *in vacuo*. The polymer yield was determined gravimetrically.

Measurements

^{1}H and ^{13}C NMR spectra were obtained using an EX-400 spectrometer (JEOL Ltd.) operated at 400 MHz for ^{1}H and 100 MHz for ^{13}C. The tacticity of poly(DMAAm) was determined from the ^{1}H NMR signals due to the methylene groups, in deuterated dimethyl sulfoxide (DMSO-d_6) at 150°C (Figure 1). The structure of the hydrogen bond-assisted complex was investigated via ^{13}C NMR spectra in toluene-d_8 at low temperatures. Molecular weights and molecular weight distributions of the polymers were determined by size exclusion chromatography (SEC); the chromatograph was calibrated with standard polystyrene samples. SEC was performed with an HLC 8220 chromatograph (Tosoh Co.) equipped with TSK gel columns (SuperHM-M (6.5 mm IDx150 mm) and SuperHM-H (6.5 mm IDx150 mm) (Tosoh Co.)). Dimethylformamide containing LiBr (10 mmol L^{-1}) was used as eluent at 40°C with flow rate 0.35 mL min^{-1}. The polymer concentration was 1.0 mg mL^{-1}.

<Figure 1>

RESULTS AND DISCUSSION

Radical Polymerization of DMAAm in Toluene at Low Temperatures

To examine the effect of polymerization temperature on stereospecificity, radical polymerization of DMAAm in the presence or absence of twofold amounts of chiral tartrates was carried out in toluene at low temperatures (Table 1, Runs 1-20). In the absence of tartrates (Table 1, Runs 1-5), the *m* dyad content increased with decreasing temperature and reached 73% at –80°C. This result corresponds with the finding in the literature.[7] On the other hand, the *r* dyad content increased with addition of tartrates and that tendency was enhanced with decreased temperature, regardless of the ester groups of the added tartrates (Table 1, Runs 6-20). Of the tartrates examined L-BuTar exhibited the best performance as a syndiotactic-specificity inducer. The *r* dyad content of the resulting polymer reached 68% on lowering the temperature to –80°C.

<Table 1>

To evaluate the differences in activation enthalpy ($\Delta H_i^{\ddagger}$–$\Delta H_s^{\ddagger}$) and activation entropy ($\Delta S_i^{\ddagger}$–$\Delta S_s^{\ddagger}$) for isotactic and syndiotactic propagation, we used Fordham's plots for DMAAm polymerization in toluene at low temperatures in the presence or absence of tartrates (Figure 2). The values were determined from the linear dependences according to equation (1):[26]

$$\ln\left(\frac{P_i}{P_s}\right) = \frac{\Delta S_i^{\ddagger} - \Delta S_s^{\ddagger}}{R} - \frac{\Delta H_i^{\ddagger} - \Delta H_s^{\ddagger}}{RT} \quad (1)$$

where P_i and P_s denote the mole fractions of isotactic and syndiotactic dyads,

respectively. For DMAAm polymerization in the presence of tartrates, plots for the temperature range –60 to 0°C were used, because the plots for –80°C deviated slightly from linear dependence. The values obtained are summarized in Table 2, together with those for NIPAAm polymerization in the presence of Lewis bases. In the case of NIPAAm isotactic-[14] or syndiotactic-specificity[12] was induced through hydrogen bond-assisted complex formation.

<Figure 2>

<Table 2>

The absolute values of $\Delta H_i^{\ddagger}-\Delta H_s^{\ddagger}$ for DMAAm polymerization in the presence or absence of tartrates were comparable with those for NIPAAm polymerization in the presence of Lewis bases. On the other hand, the absolute values of $\Delta S_i^{\ddagger}-\Delta S_s^{\ddagger}$ for DMAAm polymerization were closer to those for NIPAAm polymerization in the presence of PNO derivatives than in the presence of HMPA, regardless of the presence of tartrates. We have proposed that in the former system isotactic-specificity was induced with conformational limitation near the propagating chain-end through hydrogen-bonding interaction[14(b)], whereas in the latter system syndiotactic-specificity was induced by steric repulsion between HMPA molecules binding near the propagating chain-end[12(b)]. Thus it is assumed that the stereospecificity of DMAAm polymerization was induced by conformation near the propagating chain-end being limited. The mechanism is discussed in detail below.

The effect of the amount of L-BuTar added was examined at –60°C (Table 1, runs 4, 19, 21-23), because the plots for –80°C deviated slightly from the Fordham dependence. Figure 3 shows the relationship between $[\text{L-BuTar}]_0/[\text{DMAAm}]_0$ ratio and the *r* dyad content of the polymers obtained at $[\text{DMAAm}]_0$=0.5 mol L^{-1}. The syndiotacticity gradually increased with the $[\text{L-BuTar}]_0/[\text{DMAAm}]_0$ ratio and became almost constant for $[\text{L-BuTar}]_0/[\text{DMAAm}]_0>1$.

The effect of variation of $[\text{DMAAm}]_0$ was examined at –60°C (Table 1, runs 4, 24-26). Figure 4 displays the relationship between $[\text{L-BuTar}]_0/[\text{DMAAm}]_0$ ratio and the *r* dyad content of the polymers obtained at $[\text{L-BuTar}]_0$=1.0 mol L^{-1}. The syndiotacticity further increased slightly for $[\text{L-BuTar}]_0/[\text{DMAAm}]_0>1$ and reached 69% in the presence of a tenfold excess of L-BuTar.

<Figure 3>

<Figure 4>

Structure of the Hydrogen Bond-Assisted Complex of DMAAm with Tartrates

As reported previously,[21] the use of polar solvents such as tetrahydrofuran decreased the syndiotactic-specificity induced by tartrates. Such a solvent effect suggested that hydrogen bonding interaction plays an important role in inducing syndiotactic-specificity in DMAAm polymerization in the presence of tartrates. The following three complexes can be postulated in this polymerization system. (**A**), 1:1 complex with double hydrogen bonds; (**B**), 1:1 complex with a single hydrogen bond; (**C**), 2:1 complex with single

hydrogen bond.

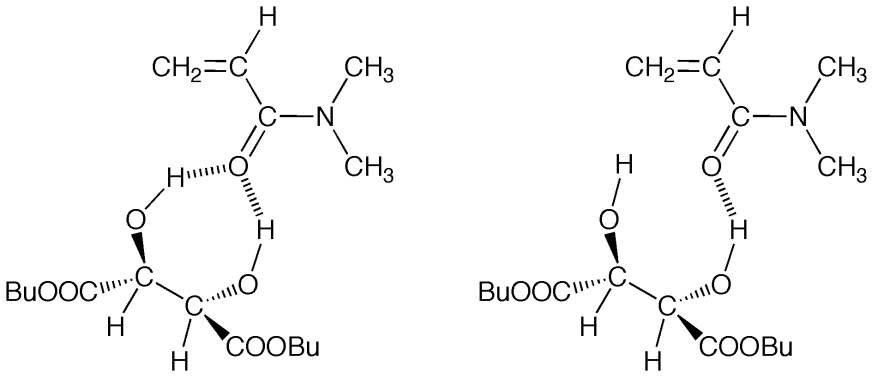

A **B**

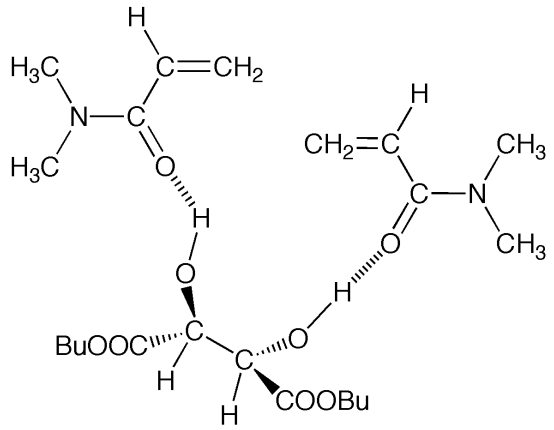

C

To investigate the stoichiometry of the DMAAm-L-BuTar complex, ^{13}C NMR analysis was carried out on solutions with $[DMAAm]_0+[L\text{-}BuTar]_0=0.25$ mol L^{-1}, in toluene-d_8 at 0°C. The upper plots in Figure 5 display changes in the chemical shift of the methylene carbon of DMAAm resulting from variation of the initial proportion of DMAAm. The plots roughly obeyed a quadratic equation. Thus the stoichiometry of the complex was evaluated by Job's method (Figure 5) via equation (2):[27]

$$[\text{DMAAm-L-BuTar}] = \frac{\delta(CH_2{=}) - \delta(CH_2{=})_f}{\delta(CH_2{=})_c - \delta(CH_2{=})_f} \times [\text{DMAAm}]_0 \quad (2)$$

where $\delta(CH_2=)$, $\delta(CH_2=)_f$ and $\delta(CH_2=)_c$ are the chemical shifts of the sample mixture, DMAAm alone and the saturated mixture, respectively. The maximum was observed at an initial proportion of DMAAm=0.5, indicating 1:1 complex formation between DMAAm and L-BuTar. This result is in accordance with the observation that an equimolar amount of L-BuTar is required to induce significant syndiotactic-specificity (cf. Figure 3).

<Figure 5>

To distinguish between structures **A** and **B** Job's method was used for solutions with $[DMAAm]_0+[-OH]_0=0.25$ mol L^{-1}, in toluene-d_8 at 0°C, to determine the mode of hydrogen bonding interaction in the DMAAm-L-BuTar complex. If the complex favors structure **B**, the maximum should be observed at initial proportion of DMAAm=0.5, whereas for structure A the maximum should correspond to initial proportion of DMAAm=0.33. Figure 6 displays changes in the chemical shift of the methylene carbon of DMAAm and Job's plots. The results differed from the predictions of both hypotheses; a broad maximum was observed for an initial proportion of DMAAm between 0.33 and 0.6.

<Figure 6>

It has been reported that L-tartrates favor the *trans* conformation even in

solution.[28] In that conformation, the two hydroxyl groups of L-tartrates should be located on the same side, which is convenient for the formation of a double hydrogen-bonding interaction with one Lewis base. Taking into account that the hypotheses above are based on the assumption that the two hydroxyl groups independently form hydrogen bonds, it is assumed that the two hydroxyl groups in L-BuTar behave like a mono-functional group. In other words, DMAAm and L-BuTar would directly form structure **A,** bypassing structure **B**.

Equilibrium Constant for the DMAAm-L-BuTar Complex

Figure 7 shows the relationship between the change in the ^{13}C NMR chemical shift of the methylene carbon of DMAAm and $[\text{L-BuTar}]_0/[\text{DMAAm}]_0$ ratio at constant $[\text{DMAAm}]_0$ ($5.0\text{x}10^{-2}$ mol L^{-1}) in toluene-d_8 at several temperatures. The equilibrium constant (K) of the DMAAm-L-BuTar complex was determined from the data in Figure 7 by nonlinear least-squares fitting to equation (3):[29]

$$\Delta\delta = \frac{\Delta\delta'}{2}\left(b - \sqrt{b^2 - 4X}\right) \qquad (3)$$

$$b = 1 + X + \frac{1}{(K[\text{DMAAm}]_0)}$$

$$X = \frac{[\text{L-BuTar}]_0}{[\text{DMAAm}]_0}$$

where $\Delta\delta$ and $\Delta\delta'$ are the changes in the chemical shift of the methylene carbon of DMAAm for the given solution and a saturated solution, respectively (Table 3).

<Figure 7>

<Table 3>

van't Hoff plots for the *K* values are shown in Figure 8. The enthalpy (ΔH) and entropy (ΔS) for complex formation were determined from equation (4):

$$\ln K = \frac{\Delta S}{R} - \frac{\Delta H}{RT} \quad (4)$$

where *R* is the gas constant (8.315 J mol^{-1} K^{-1}) and *T* is the absolute temperature (K). The values are summarized in Table 4 together with those for the NIPAAm-HMPA complex. Although the basicity of the amide carbonyl is lower than that of HMPA, and the acidity of the alcohol –OH is lower than that of the amide –NH, ΔH for the DMAAm-L-BuTar complex was found to be comparable with that for the NIPAAm-HMPA complex. Furthermore, ΔS for the DMAAm-L-BuTar complex was found to be much smaller than for the NIPAAm-HMPA complex, suggesting a large reduction in degrees of freedom by formation of the DMAAm-L-BuTar complex compared with the NIPAAm-HMPA complex. These results support structure **A**, i.e. 1:1 complex with double hydrogen bonds.

<Figure 8>

<Table 4>

Application of the *K* values for the polymerization conditions (cf. Table 1, runs 16-20) gives the values shown in Table 3 for the degree of association (α) of DMAAm.

The DMAAm monomer formed the complex quantitatively at lower temperatures, whereas 13% of DMAAm was uncomplexed at 0°C. This result corresponds with the temperature dependence of the syndiotactic-specificity of DMAAm polymerization in the presence of L-BuTar (cf. Figure 1).

Proposed Mechanism for the Stereospecific DMAAm Polymerization

As noted above, isotactic polymer was obtained by radical polymerization of DMAAm in toluene at low temperatures in the absence of tartrates, whereas most atactic polymer was obtained by radical polymerization of *N*-methylacrylamide (NMAAm) under corresponding conditions.[16] This indicates that the methyl group *trans* to the carbonyl group of DMAAm plays an important role in inducing isotactic-specificity.

The low stereospecificity in NMAAm polymerization is attributable to free rotation near the propagating chain-end reducing the steric repulsion between the amide moieties at the penultimate and chain-end monomeric units (Scheme 1).[12(b)] The rotated radicals can react with a new incoming monomer via two possible pathways. Thus atactic polymers were obtained in the NMAAm polymerization, because pathway **a** forms an *r* dyad and pathway **b** an *m* dyad.

<Scheme 1>

In the DMAAm polymerization, rotation around backbone bonds near the second dyad from the chain-end and the chain-end would take place, because steric

repulsion between the methyl groups *trans* to the carbonyl groups at the antepenultimate and penultimate monomeric units arises. Thus the conformation near the propagating chain-end would be determined by steric repulsion between the amide moieties at the antepenultimate, penultimate and chain-end monomeric units (Scheme 2). The steric hindrance of the amide moiety at the penultimate monomeric unit would limit approach via pathway **a** of the next incoming monomer, resulting in the formation of isotactic polymer.

<Scheme 2>

In DMAAm polymerization in the presence of tartrates, the propagating chain-end becomes more crowded due to the formation of the double hydrogen bonds between the added tartrates and the carbonyl groups of monomeric units near the chain-end. Thus the conformation near the propagating chain-end would be determined by steric repulsion between not only the amide moieties but also the tartrates. It is assumed that the tartrate complexing at the antepenultimate monomeric unit is crowded out to the front free-space to reduce steric repulsion (Scheme 2). If so, steric hindrance of the tartrates at the antepenultimate monomeric unit would limit approach via pathway **b** of the next incoming monomer. As a result, syndiotactic-specificity was induced.

Effect of Optical Activity of Added Tartrates on the Syndiotactic Specificity of DMAAm Polymerization

To examine the effect of optical activity of added tartrates on syndiotactic-specificity, DMAAm polymerization was carried out in the presence of D-EtTar or *rac*-EtTar (Table 5). D-EtTar induced syndiotactic-specificity as well as L-EtTar (Table 1, Runs 6-10 and Table 5, Runs 1-5). However, a slight decrease in the syndiotacticity of the polymer was observed when *rac*-EtTar was added at lower temperatures such as –60 and –80°C (Table 5, Runs 9 and 10). DMAAm polymerization was then carried out at –60°C in the presence of mixtures of L-EtTar and D-EtTar (Figure 9). Mixing the enantiomers reduced the syndiotacticity and the molecular weight of the polymers formed, regardless of the relative proportions of L-EtTar and D-EtTar (Table 1, Run 9 and Table 5, Runs 4, 9, 11, 12).

<Table 5>

<Figure 9>

The ^{13}C NMR signals due to carbonyl carbons and β-carbons of DMAAm monomer showed downfield shifts with the addition of L-EtTar or *rac*-EtTar, when measured in toluene-d_8 at –60°C (Figure 10a-c). Furthermore, mixtures of DMAAm with L-EtTar and *rac*-EtTar showed almost the same spectral patterns (Figure 10b and c). These results indicate that DMAAm-EtTar complex formation is independent of the optical activity of the added tartrates, and suggests that the optical activity of the added tartrates affects the stereoselectivity of the propagating radicals. As proposed above, the added tartrates should bind to the carbonyl groups of monomeric units near the

syndiotactic-specific propagating chain-end (cf. Scheme 2). If the tartrate binding to the penultimate monomeric unit is changed from L-EtTar to D-EtTar, the propagating radical is the diastereomer of the original species. If steric repulsion between the racemic tartrates near the chain-end is stronger than between the chiral tartrates, the tartrates binding near the propagating chain-end would be released. The release of tartrates would reduce the syndiotactic-specificity, because the steric balance near the chain-end should be responsible for the induction of syndiotactic-specificity.

<Figure 10>

We conducted ^{13}C NMR analysis of mixtures of poly(DMAAm) and EtTar (Figures 10d and e). Signals due to poly(DMAAm) were not detected, probably because poor mobility of poly(DMAAm) at –60°C resulted in broadening of its signals. The signals due to EtTar were observed, although they were broad compared with those of the DMAAm-EtTar complexes (Figure 10b and c), suggesting complex formation between the added tartrates and the amide groups in poly(DMAAm). Furthermore, the signals due to L-EtTar were broader than those due to *rac*-EtTar, suggesting that L-EtTar binds to poly(DMAAm) more strongly than *rac*-EtTar. These results support the above-mentioned hypothesis.

DMAAm Polymerization in the presence of *meso*-BuTar

DMAAm polymerization was conducted in the presence of *meso*-BuTar to investigate the

effect of the configuration of the added tartrates (Table 1, Run 27). The molecular weight of the polymer obtained hardly varied even with the addition of *meso*-BuTar, although significant increases were observed in the presence of chiral tartrates. Furthermore, the induced syndiotactic-specificity was lower and between those with L-BuTar and a monoalcohol compound, such as D-EtMal (Table 1, Run 28). It is known that the dimethyl ester of *meso*-tartaric acid prefers chiral conformations in the crystalline state[30] as well as *meso*-tartaric acid[31] and its salts.[32] This conformation is advantageous for the formation of 1:1 complex with double hydrogen bonds as per structure **A**. However, unlike L-BuTar, the conformation of *meso*-BuTar in solution would vary rapidly, taking into account that *meso*-tartaric acid is optically inactive in solution because the preferred conformations equilibrate .[33] Thus it is assumed that complex formation between DMAAm and *meso*-BuTar was suppressed owing to the rapid equilibrium in the conformation of *meso*-BuTar[34] so that the induced syndiotactic-specificity was lower than with L-BuTar.

CONCLUSION

The radical polymerization of DMAAm in the presence of tartrates was investigated. We succeeded in synthesizing poly(DMAAm) with r=69% by lowering the monomer concentration to 0.1 mol L^{-1} at –60°C. The syndiotacticity is the highest value for radically prepared poly(DMAAm)s. NMR analysis suggests that formation of a hydrogen bond-assisted complex with double hydrogen bonds is the key to induction of syndiotactic-specificity. Further work is under way to examine in detail the effect of the

N-substituents on the stereospecificity of radical polymerization of *N*,*N*-disubstituted acrylamides in the presence of chiral tartrates.

This work was supported in part by a Grant-in-Aid for Young Scientists (B) (18750102) from the Ministry of Education, Culture, Sports, Science and Technology.

REFERENCES AND NOTE

1. (a) Yuki, H.; Hatada, K.; Niinomi, Y.; Kikuchi, Y. Polym J 1970, 1, 36–45. (b) Nakano, T.; Matsuda, A.; Okamoto, Y. Polym J 1996, 28, 556–558. (c) Nakano, T.; Shikisai, Y.; Okamoto, Y. Polym J 1996, 28, 51-60.
2. (a) Isobe, Y.; Yamada, K.; Nakano, T.; Okamoto, Y. Macromolecules 1999, 32, 5979-5981. (b) Isobe, Y.; Yamada, K.; Nakano, T.; Okamoto, Y. J Polym Sci: Part A: Polym Chem 2000, 38, 4693-4703.
3. (a) Miura, Y.; Satoh, T.; Narumi, A.; Nishizawa, O.; Okamoto, Y.; Kakuchi, T. Macromolecules 2005, 38, 1041-1043. (b) Miura, Y.; Satoh, T.; Narumi, A.; Nishizawa, O.; Okamoto, Y.; Kakuchi, T. J Polym Sci: Part A: Polym Chem 2006, 44, 1436-1446.
4. Kaneko, Y.; Iwakiri, N.; Sato, S.; Kadokawa, J. Macromolecules 2008, 41, 489-492.
5. Yamada, K.; Nakano, T.; Okamoto, Y. Macromolecules 1998, 31, 7598-7605.
6. (a) Porter, N. A.; Allen, T. R.; Breyer R. A, J Am Chem Soc 1992, 114, 7676-7683. (b) Wu, W.-X., McPhail, A. T.; Porter, N. A. J Org Chem 1994, 59, 1302-1308.
7. Liu, W.; Nakano, T.; Okamoto, Y. Polym J 2000, 32, 771-777.

8. (a) Isobe, Y.; Fujioka, D.; Habaue, S.; Okamoto, Y. J Am Chem Soc 2001, 123, 7180-7181. (b) Habaue, S.; Isobe, Y.; Okamoto, Y. Tetrahedron 2002, 58, 8205-8209.

9. (a) Ray, B.; Isobe Y.; Morioka, K.; Habaue, S.; Okamoto, Y.; Kamigaito, M.; Sawamoto, M. Macromolecules 2003, 36, 543-545. (b) Ray, B.; Isobe Y.; Matsumoto, K.; Habaue, S.; Okamoto, Y.; Kamigaito, M.; Sawamoto, M. Macromolecules 2004, 37, 1702-1710.

10. (a) Lutz, J.-F.; Neugebauer, D.; Matyjaszewski, K. J Am Chem Soc 2003, 125, 6986-6993. (b) Lutz, J.-F.; Jakubowski, W.; Matyjaszewski, K. Macromol Rapid Commun. 2004, 25, 486-492.

11. (a) Hoshikawa, N.; Hotta, Y.; Okamoto, Y. J Am Chem Soc 2003, 125, 12380-12381. (b) Azam, A. K. M. F.; Kamigaito, M.; Okamoto, Y. Polym J 2006, 38, 1035-1042. (c) Azam, A. K. M. F.; Kamigaito, M.; Okamoto, Y. J Polym Sci: Part A: Polym Chem 2007, 45, 1304-1315.

12. (a) Hirano, T.; Miki, H.; Seno, M.; Sato, T. J Polym Sci: Part A: Polym Chem 2004, 42, 4404-4408. (b) Hirano, T.; Miki, H.; Seno, M.; Sato T. Polymer 2005, 46, 3693-3699. (c) Hirano, T.; Miki, H.; Seno, M.; Sato T. Polymer 2005, 46, 5501-5505.

13. (a) Hirano, T.; Ishii, S.; Kitajima, H.; Seno, M.; Sato, T. J Polym Sci: Part A: Polym Chem 2005, 43, 50-62. (b) Hirano, T.; Kitajima, H.; Ishii, S.; Seno, M.; Sato, T. J Polym Sci: Part A: Polym Chem 2005, 43, 3899-3908. (c) Hirano, T.; Kitajima, H.; Seno, M.; Sato T. Polymer 2006, 47, 539-546.

14. (a) Hirano, T.; Ishizu, H.; Seno, M.; Sato T. Polymer 2005, 46, 10607-10610. (b) Hirano, T.; Ishizu, M.; Sato T. Polymer 2008, 49, 438-445.

15. (a) Hirano, T.; Okumura, Y.; Kitajima, H.; Seno, M.; Sato, T. J Polym Sci: Part A: Polym Chem 2006, 44, 4450-4460. (b) Hirano, T.; Kamikubo, T.; Okumura, Y.; Sato, T. Polymer 2007, 48, 4921-4925. (c) Hirano, T.; Kamikubo, T.; Fujioka, Y.; Sato, T. Eur Polym J 2008, 44, 1053-1059.

16. Hirano, T.; Nakamura, K.; Kamikubo, T.; Ishii, S.; Tani, K.; Mori, T.; Sato, T. J Polym Sci: Part A: Polym Chem 2008, 46, 4575-4583.

17. Hirano, T.; Miyazaki, T.; Ute, K. J Polym Sci: Part A: Polym Chem 2008, 46, 5698-5701.

18. Wan, D.; Satoh, K.; Kamigaito, M. Macromolecules 2006, 39, 6882-6886.

19. Wan, D.; Satoh, K.; Kamigaito, M.; Okamoto, Y. Macromolecules 2005, 38, 10397-10405.

20. Hirano, T.; Okumura, Y.; Seno, M.; Sato, T. Eur Polym J 2006, 42, 2114-2124.

21. Hirano, T.; Masuda, S.; Sato, T. J Polym Sci: Part A: Polym Chem 2008, 46, 3145-3149.

22. (a) Xie, X.; Hogen-Esch, T. E. Macromolecules 1996, 29, 1746-1752. (b) Kobayashi, M.; Okuyama, S.; Ishizone, T.; Nakahama, S. Macromolecules, 32, 6466-6477. (c) Kobayashi, M.; Ishizone, T.; Nakahama, S. Macromolecules, 33, 4411-4416.

23. Ning, Y.; Zhu, H.; Chen, E. Y.-X. J Organomet Chem 2007, 692, 4535-4544.

24. Dupau, P.; Epple, R.; Thomas, A. A.; Fokin, V. V.; Sharpless, K. B. Adv Synth Catal 2002, 344, 421-433.

25. Zhang, Z.; Chung, T. C. M. Macromolecules 2006, 39, 5187-5189.

26. Fordham, J. W. L. J Polym Sci 1959, 39, 321-334.

27. Gil, V. M. S.; Oliveira, N. C. J Chem Educ 1990, 67, 473-478.

28. (a) Polavarapu, P. L.; Ewig, C. S.; Chandramouly, T. J Am Chem Soc 1987, 109, 7382-7386. (b) Egli, M.; Dobler, M. Helv Chim Acta 1989, 72, 1136-1150. (c) Gawronski, J.; Gawronska, K.; Skowronek, P.; Rychlewska, U.; Warzajtis, B.; Rychlewski, J.; Hoffmann, M.; Szarecka, A. Tetrahedron 1997, 53, 6113-6144.

29. Macomber, R. S. J Chem Educ 1992, 69, 375-378.

30. Kroon, J.; Kanters, J. A. Acta Cryst 1973, B29, 1278-1283.

31. Bootsma, G. A.; Schoone, J. C. Acta Cryst 1967, 22, 522-532.

32. (a) Kroon, J.; Peerdeman, A. F.; Bijvoet, J. M. Acta Cryst 1965, 19, 293-297. (b) Kroon, J.; Kanters, J. A. Acta Cryst 1972, B28, 714-722.

33. Ascenso, J.; Gil, V. M. S. Can J Chem 1980, 58, 1376-1379.

34. Downfield shift of C=O NMR signal of DMAAm (0.125 mol L^{-1}, in toluene-d_8 at –60°C) with the addition of twofold amount of meso-BuTar (0.88 ppm) was smaller than that with L-BuTar (1.43 ppm). This result suggests that C=O group of DMAAm form hydrogen bonding with meso-BuTar less than L-BuTar, probably because of rapid equilibrium in the conformation of *meso*-BuTar.

Table 1. Radical Polymerization of DMAAm in Toluene at Low Temperatures for 24 h in the Presence or Absence of Tartrates[a]

Run	Added Tartrate	Temp. °C	$[DMAAm]_0$ mol L^{-1}	$\frac{[Tartrate]_0}{[DMAAm]_0}$	Yield %	Dyad / %[b] *m*	*r*	M_n[c] x 10^4	$\frac{M_w}{M_n}$[c]
1	None	0	0.50	0.0	82	62	38	1.21	1.5
2	None	–20	0.50	0.0	77	64	36	1.39	1.5
3	None	–40	0.50	0.0	41	66	34	1.50	1.6
4	None	–60	0.50	0.0	56	70	30	2.21	1.6
5	None	–80	0.50	0.0	62	73	27	5.20	1.8
6	L-EtTar	0	0.50	2.0	>99	46	54	1.72	2.1
7	L-EtTar	–20	0.50	2.0	>99	43	57	2.40	2.2
8	L-EtTar	–40	0.50	2.0	>99	40	60	3.37	2.6
9[d]	L-EtTar	–60	0.50	2.0	>99	37	63	7.70	3.0
10[d]	L-EtTar	–80	0.50	2.0	>99	37	63	12.8	2.3
11	L-iPrTar	0	0.50	2.0	>99	48	52	1.71	2.0
12	L-iPrTar	–20	0.50	2.0	>99	41	59	2.36	2.6
13	L-iPrTar	–40	0.50	2.0	>99	38	62	3.88	2.6
14[d]	L-iPrTar	–60	0.50	2.0	>99	35	65	7.38	2.7
15[d]	L-iPrTar	–80	0.50	2.0	>99	34	66	9.10	2.8
16	L-BuTar	0	0.50	2.0	>99	45	55	1.92	2.4
17	L-BuTar	–20	0.50	2.0	>99	40	60	3.51	2.4
18	L-BuTar	–40	0.50	2.0	>99	36	64	7.60	2.3
19[d]	L-BuTar	–60	0.50	2.0	>99	34	66	6.73	3.2
20[d]	L-BuTar	–80	0.50	2.0	>99	32	68	8.65	3.3
21	L-BuTar	–60	0.50	0.20	93	57	43	3.37	1.5
22	L-BuTar	–60	0.50	0.50	>99	45	55	3.87	2.1
23[d]	L-BuTar	–60	0.50	1.0	>99	37	63	4.65	2.9
24[d]	L-BuTar	–60	0.10	10	>99	31	69	2.20	2.1
25[d]	L-BuTar	–60	0.25	4.0	>99	32	68	5.00	2.9
26	L-BuTar	–60	1.0	1.0	>99	37	63	8.89	3.8
27[d]	*meso*-BuTar	–60	0.50	2.0	>99	49	51	1.88	2.2
28[e]	D-EtMal	–60	0.50	4.0	>99	59	41	1.88	1.9

a. $[n\text{-}Bu_3B]_0$=0.05 mol L^{-1}.

b. Determined by ^1H NMR signals due to methylene group.

c. Determined by SEC (polystyrene standards).

d. Monomer, polymer or both precipitated during polymerization reaction.

e. $[D\text{-}EtMal]_0$=2.0 mol L^{-1}.

Table 2. Activation Parameters for Radical Polymerization of DMAAm and NIPAAm in the Presence or Absence of Stereocontrolling Auxiliaries

Monomer	Added Agent	$\Delta H_i^{\ddagger}$-$\Delta H_s^{\ddagger}$ kJ mol^{-1}	$\Delta S_i^{\ddagger}$-$\Delta S_s^{\ddagger}$ J mol^{-1} K^{-1}
DMAAm	None	–2.84±0.14	–6.4±0.6
DMAAm	L-EtTar	2.99±0.14	9.5±0.6
DMAAm	L-iPrTar	4.14±0.85	13.9±3.5
DMAAm	L-BuTar	3.71±0.65	11.5±2.7
NIPAAm[a]	None	–0.36±0.36	–2.8±1.5
NIPAAm[a]	HMPA	2.31±0.09	3.7±0.3
NIPAAm[b]	35DMPNO	–4.76±0.68	–15.7±2.8

a. Data from ref. 12(b).

b. Data from ref. 14(b).

Table 3. Equilibrium Constants (*K*) for the Interaction between DMAAm and L-BuTar and Degree of Association (α) in the Polymerization System[a]

Temperature °C	*K*/L mol^{-1}	α[b]
25	5.47	-
0	12.1	0.87
–20	22.9[c]	0.92
–40	50.0	0.96
–60	130[c]	0.99
–80	409[c]	1.00

a. NMR conditions: $[DMAAm]_0=5.0\times10^{-2}$ mol L^{-1}, toluene-d_8.

b. Calculated with $[DMAAm]_0=0.50$ mol L^{-1} and $[L\text{-BuTar}]_0=1.0$ mol L^{-1}.

c. Calculated from van't Hoff relationship.

Table 4. Enthalpy and Entropy for Hydrogen Bond-Assisted Complex Formation

Complex System	ΔH kJ mol^{-1}	ΔS J mol^{-1} K^{-1}
DMAAm-L-EtTar	–19.5±0.7	–51.2±2.5
NIPAAm-HMPA[a]	–18.5±0.8	–35.8±2.8

a. Data from ref. 12(b).

Table 5. Radical Polymerization of DMAAm in Toluene at Low Temperatures for 24h in the Presence of EtTar[a]

Run	[L-EtTar]$_0$	[D-EtTar]$_0$	Temp.	Yield	Dyad / %[b]		M_n[c]	M_w[c]
	mol L^{-1}	mol L^{-1}	°C	%	*m*	*r*	x 10^4	M_n
1	0.0	1.0	0	>99	45	55	2.44	1.7
2	0.0	1.0	–20	>99	45	55	2.90	1.9
3	0.0	1.0	–40	>99	42	58	4.43	2.1
4	0.0	1.0	–60	>99	36	64	7.44	2.6
5[d]	0.0	1.0	–80	>99	36	64	4.73	2.1
6	0.5	0.5	0	>99	45	55	2.44	1.7
7	0.5	0.5	–20	97	44	56	2.32	2.1
8	0.5	0.5	–40	>99	42	58	3.96	2.3
9	0.5	0.5	–60	>99	44	56	2.52	2.2
10[d]	0.5	0.5	–80	98	43	57	2.74	2.6
11	0.25	0.75	–60	77	42	58	2.81	3.0
12	0.75	0.25	–60	>99	43	57	2.71	2.6

a. [DMAAm]$_0$=0.5 mol L^{-1}, [*n*-Bu$_3$B]$_0$=0.05 mol L^{-1}.

b. Determined by ^{1}H NMR signals due to methylene group.

c. Determined by SEC (polystyrene standards).

d. Monomer, polymer or both precipitated during polymerization reaction.

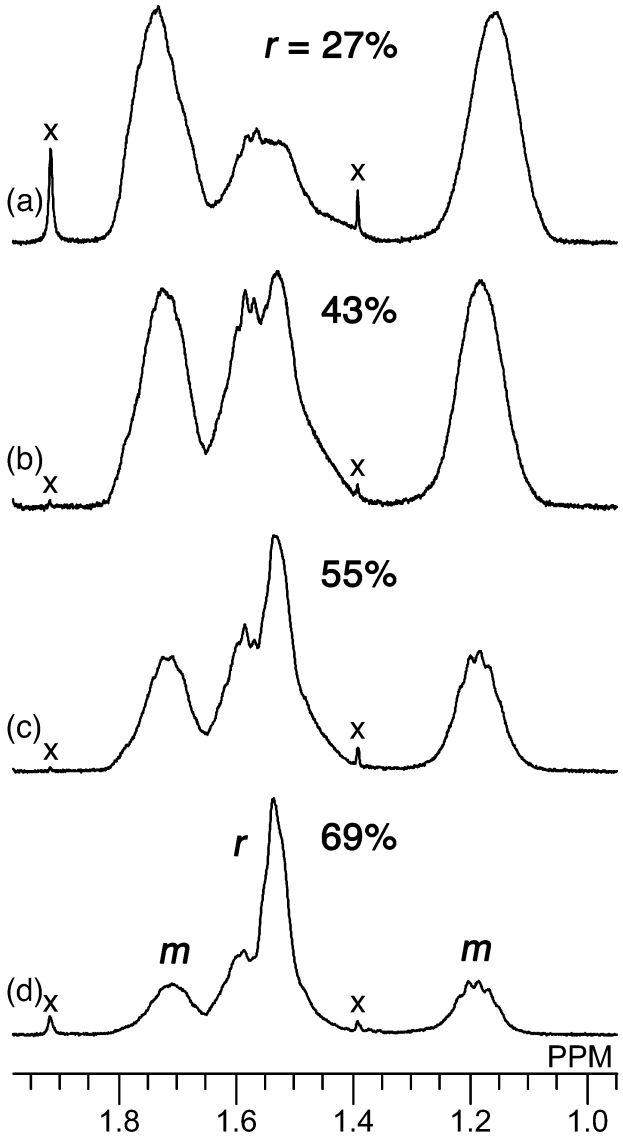

Figure 1. ^{1}H NMR spectra of the main-chain methylene groups of poly(DMAAm) with different *r* dyads, measured in DMSO-d_6 at 150°C. (a) 27%, (b) 43%, (c) 55%, (d) 69%. x denotes impurities.

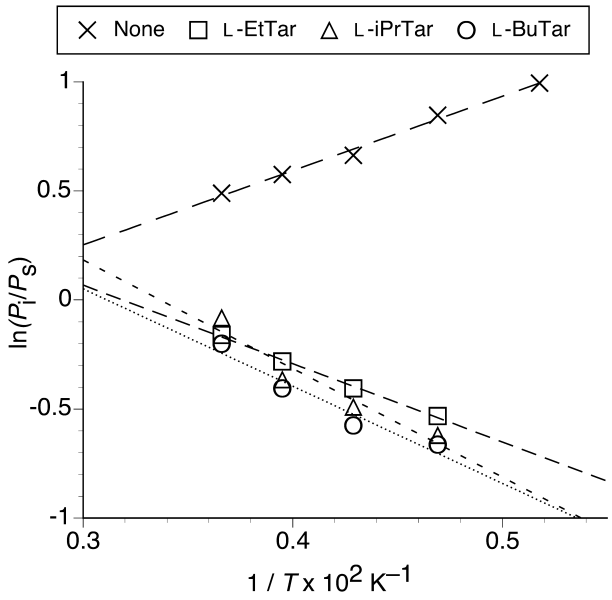

Figure 2. Fordham's plots for radical polymerization of DMAAm in toluene in the presence or absence of tartrates. P_i and P_s denote the mole fractions of isotactic and syndiotactic dyads, respectively.

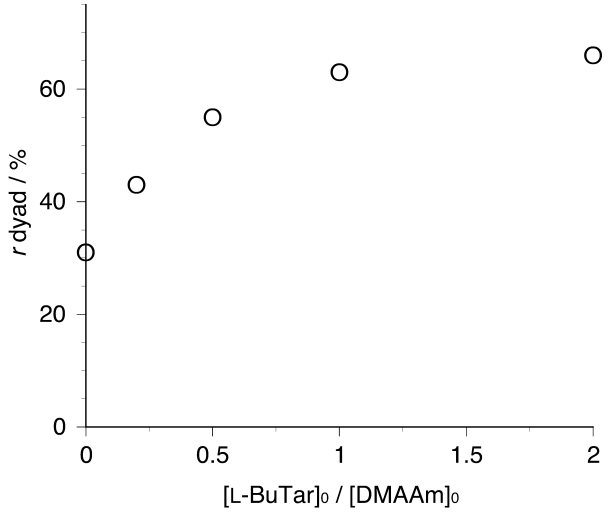

Figure 3. Relationship between $[\text{L-BuTar}]_0/[\text{DMAAm}]_0$ ratio and *r* dyad content of poly(DMAAm)s prepared in toluene at –60°C with constant initial concentration of DMAAm ($[\text{DMAAm}]_0$=0.50 mol L^{-1}).

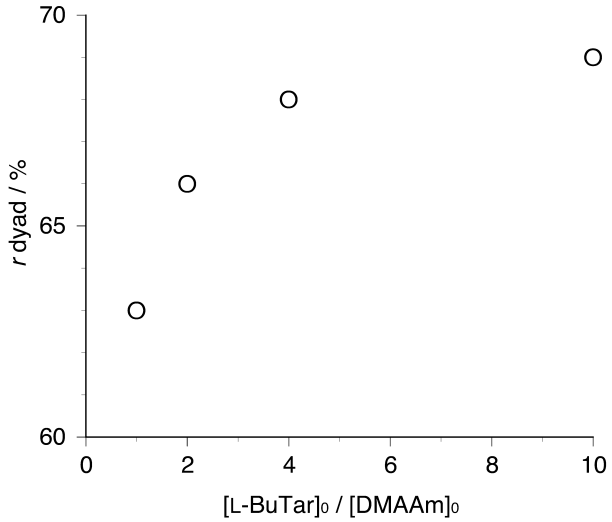

Figure 4. Relationship between $[\text{L-BuTar}]_0/[\text{DMAAm}]_0$ ratio and *r* dyad content of poly(DMAAm)s prepared in toluene at –60°C with constant concentration of L-BuTar ($[\text{L-BuTar}]_0$=1.0 mol L^{-1}).

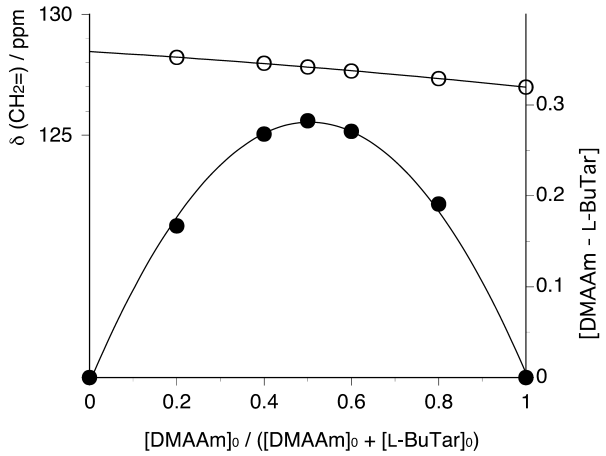

Figure 5. Job's plots of the chemical shifts of the methylene carbons of DMAAm versus the concentration of L-BuTar relative to DMAAm, and for the association of DMAAm and L-BuTar in toluene-d_8 at 0°C. $[DMAAm]_0+[L\text{-}BuTar]_0=0.25$ mol L^{-1}.

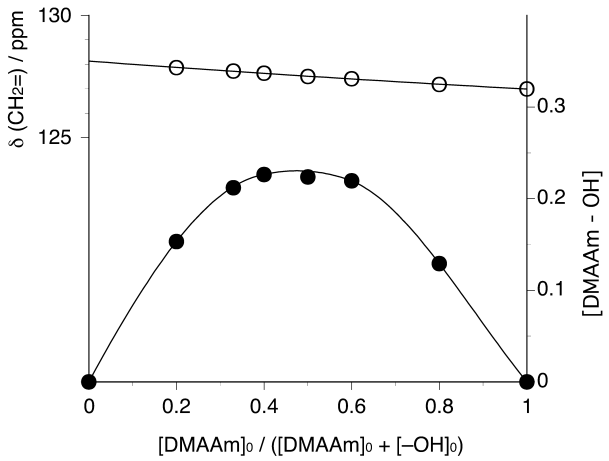

Figure 6. Job's plots of the chemical shifts of the methylene carbons of DMAAm versus the concentration of –OH group, and for the association of DMAAm and –OH group in toluene-d_8 at 0°C. $[DMAAm]_0+[–OH]_0$=0.25 mol L^{-1}.

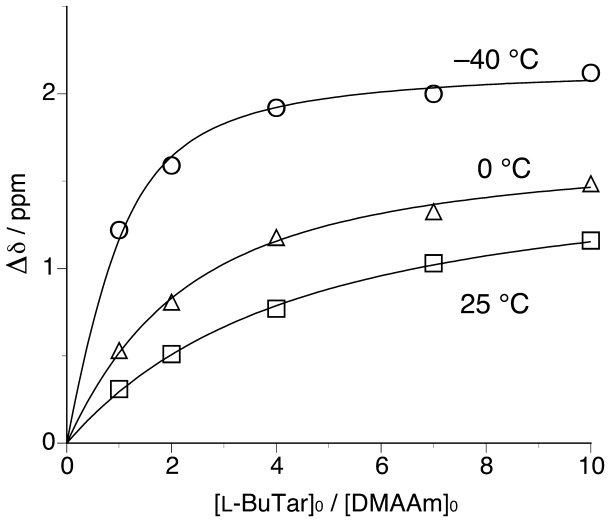

Figure 7. Changes in the chemical shifts of the methylene carbon of DMAAm with [L-BuTar]$_0$/[DMAAm]$_0$ ratio in toluene-d_8 at various temperatures.

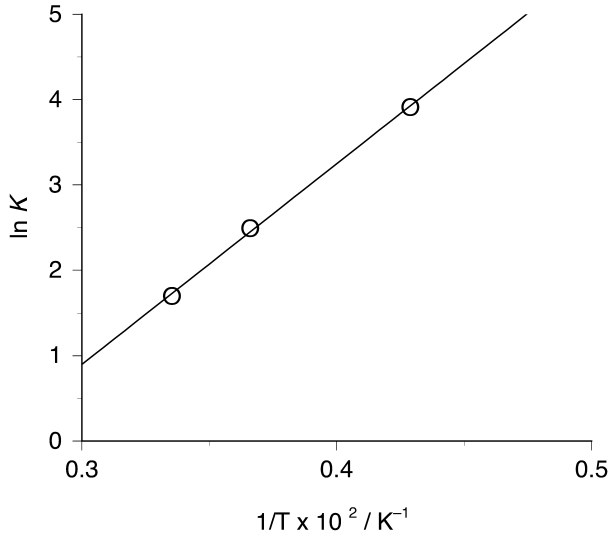

Figure 8. van't Hoff plot for 1:1 complex formation between DMAAm and L-BuTar in toluene-d_8.

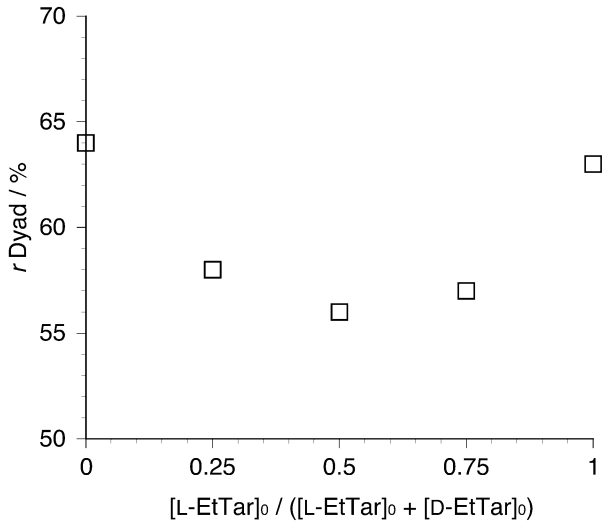

Figure 9. Relationship between the initial fraction of L-EtTar and *r* dyad content of poly(DMAAm) formed in toluene at –60°C.

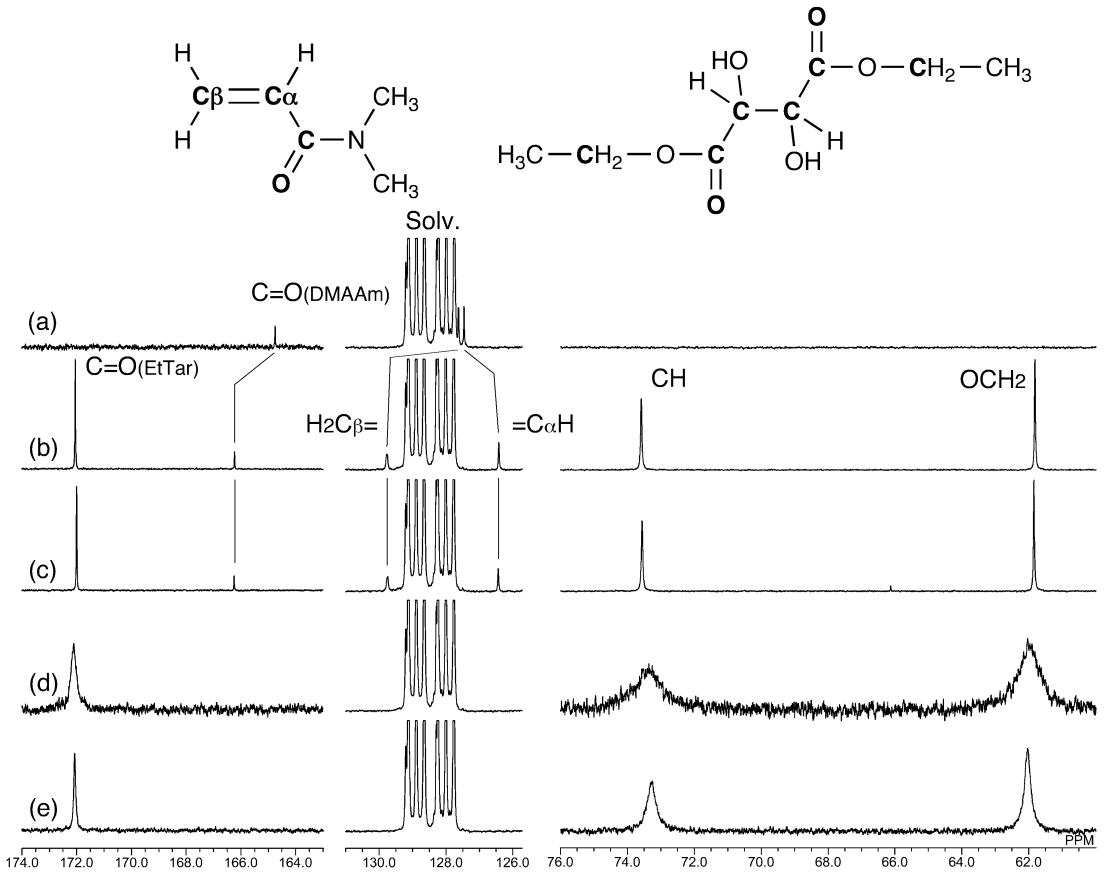

Figure 10. Expanded scale ^{13}C NMR spectra of (a), DMAAm ([DMAAm]$_0$=0.125 mol L^{-1}); (b), mixture of DMAAm and L-EtTar ([DMAAm]$_0$=0.125 mol L^{-1}, [L-EtTar]$_0$=0.25 mol L^{-1}); (c), mixture of DMAAm and *rac*-EtTar ([DMAAm]$_0$=0.125 mol L^{-1}, [*rac*-EtTar]$_0$=0.25 mol L^{-1}); (d), mixture of poly(DMAAm) and L-EtTar ([DMAAm unit]$_0$=0.125 mol L^{-1}, [L-EtTar]$_0$=0.25 mol L^{-1}); (e), mixture of poly(DMAAm) and *rac*-EtTar ([DMAAm unit]$_0$=0.125 mol L^{-1}, [*rac*-EtTar]$_0$=0.25 mol L^{-1}); measured in toluene-d_8 at –60°C.

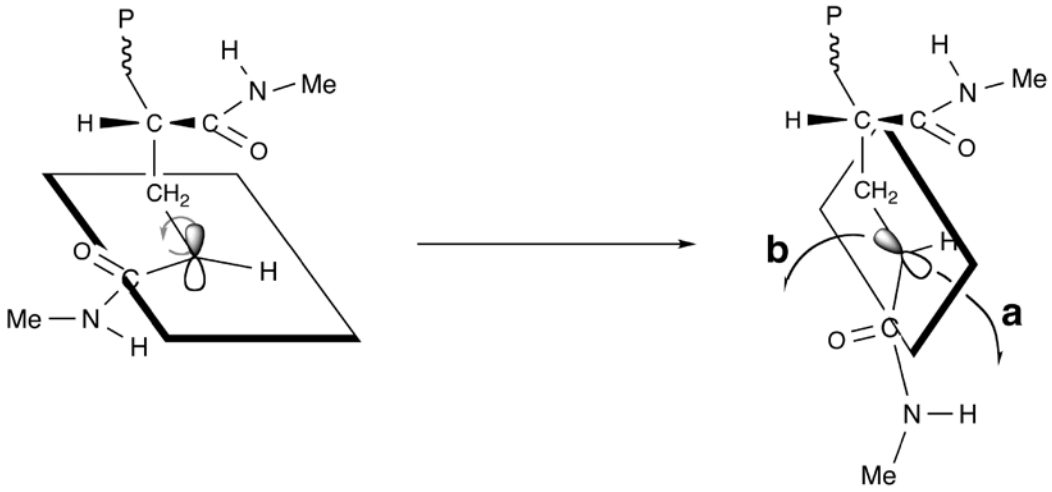

Scheme 1. Proposed mechanism for radical polymerization of NMAAm.

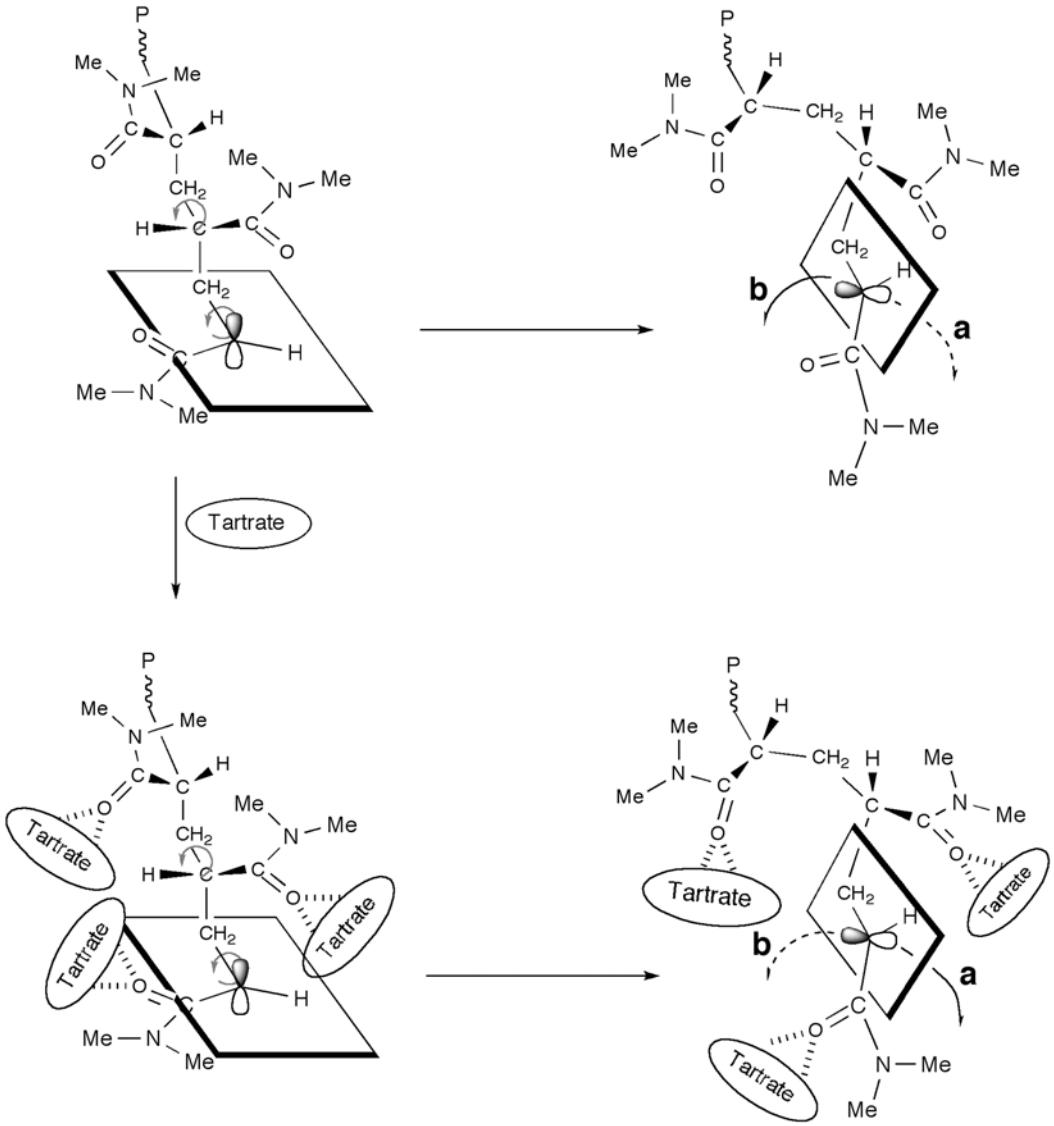

Scheme 2. Proposed mechanisms for isotactic-specific polymerization of DMAAm in the absence of tartrates, and syndiotactic-specific polymerization of DMAAm induced by tartrates.